An Iron-Dependent Alcohol Dehydrogenase Is Involved in Ethanol Metabolism of *Aromatoleum aromaticum*

Yvonne Gemmecker , Iris Schall , Andreas Seubert , Nicole Paczia , Johann Heider *

Posted Date: 7 July 2025

doi: 10.20944/preprints202507.0481.v1

Keywords: alcohol dehydrogenase; enzyme kinetics; alcohol tolerance; aliphatic alcohols; growth experiments; coupled enzyme assay

 doi:10.20944/preprints202507.0481.v1

Article

An Iron-Dependent Alcohol Dehydrogenase Is Involved in Ethanol Metabolism of *Aromatoleum aromaticum*

Yvonne Gemmecker [1], Iris Schall [1], Andreas Seubert [2], Nicole Paczia [3] and Johann Heider [1,4,*]

[1] Laboratory for Microbial Biochemistry, Philipps University of Marburg, 35043 Marburg, Germany
[2] Department of Chemistry, Philipps University Marburg, 35043 Marburg, Germany
[3] Core Facility for Metabolomics and Small Molecule Mass Spectrometry, Max Planck Institute for Terrestrial Microbiology, 35043 Marburg, Germany
[4] LOEWE-Center for Synthetic Microbiology, Marburg, Germany
* Correspondence: heider@biologie.uni-marburg.de; Tel.: +19-6421-2821527

Abstract

The NAD$^+$-dependent alcohol dehydrogenase AdhB from *Aromatoleum aromaticum* EbN1 belongs to family III of Fe-dependent alcohol dehydrogenases. It was recombinantly produced in *Escherichia coli* and biochemically characterized, showing activity only with ethanol or *n*-propanol. The enzyme contained substoichiometric amounts of Fe, Zn and Ni and a yet unidentified nucleotide-like cofactor, as indicated by mass spectrometric data. As suggested by its narrow substrate spectrum and complementation of a related species to growth on ethanol, the most probable physiological function of AdhB is the oxidation of short aliphatic alcohols such as ethanol or *n*-propanol. AdhB was also tested for its biotechnological applicability as auxiliary enzyme for the conversion of acetate to ethanol in coupled enzyme assays with the tungsten enzyme aldehyde oxidoreductase.

Keywords: alcohol dehydrogenase; enzyme kinetics; alcohol tolerance; aliphatic alcohols; growth experiments; coupled enzyme assay

1. Introduction

The betaproteobacterial species *Aromatoleum aromaticum* is highly flexible in growing on many different substrates under either aerobic or denitrifying conditions. In addition to various aromatic compounds, it also accepts aliphatic substrates, e.g., several amino acids, organic acids, aldehydes, ketones, or alcohols. The pathways involved in either aerobic or anaerobic degradation of many of these substrates have been identified in recent years, and many of the participating enzymes have been biochemically characterized. Moreover, the available genome sequence allowed us to correlate the respective enzymes with their coding genes and to investigate their induction and regulation processes in the presence or absence of the respective substrates [1–3].

In a previous study, we have observed that a constructed *A. aromaticum* strain lacking the *pdh* gene for a substrate-specific phenylacetaldehyde dehydrogenase involved in anaerobic phenylalanine (Phe) degradation showed highly retarded growth on Phe, but evolved back to almost the previous growth rate by overexpressing the *aldB* gene for another aldehyde dehydrogenase, which carried a mutation of a single amino acid (Y460C) and forms an apparent operon with the *adhB* gene coding for an Fe-dependent alcohol dehydrogenase [4]. The original *aldB* gene product was recently characterised as NAD$^+$-dependent aldehyde dehydrogenase exhibiting high activities with acetaldehyde or propionaldehyde and lower activities with benzaldehyde or phenylacetaldehyde. In contrast, the Y460C variant showed strongly reduced activities with acetaldehyde or propionaldehyde and lost its activity with benzaldehyde, but retained the same activity with

 doi:10.20944/preprints202507.0481.v1

phenylacetaldehyde as wild-type AldB [5]. Therefore, it has been assumed that the physiological role of AldB is the oxidation of the aldehyde intermediates in the degradation pathway of short aliphatic alcohols [5,6], while the co-expressed *adhB* gene in the same operon might code for the corresponding alcohol dehydrogenase. However, neither the physiological role nor the biochemical properties of AdhB have been confirmed, prompting us to purify the protein and determine its biochemical properties.

The alcohol dehydrogenases (EC 1.1.1.1) are NAD(P)$^+$ dependent enzymes oxidizing a wide range of aliphatic or aromatic alcohols to the corresponding aldehydes (or catalyzing the reverse reaction with NAD(P)H as cofactor). They are present in all organisms and typically consist of homodimers or -tetramers of 45-60 kDa subunits. Most of the known ADHs are currently affiliated to three major families: family I consists of the medium- or long-chain zinc-containing ADHs, the most studied group in vertebrates; family II, the "short-chain dehydrogenases and reductases" (SDR) do not harbor a metal cofactor; and family III is represented by the iron-dependent or iron-activated enzymes containing a transition metal ion (mostly Fe^{2+}) in the active center [7–10]. The alleged alcohol dehydrogenase AdhB of *A. aromaticum* is affiliated to the iron dependent ADHs of family III [11], representing the only enzyme of this family encoded in the genome [1].

2. Materials and Methods

Cloning, heterologous gene expression and preparation of cell-free extracts. The gene *adhB* (ebA4623) from *A. aromaticum* strain EbN1 was amplified via PCR from chromosomal DNA using appropriate primers (AdhB_for AAGCTCTTCAATGAGCACGACGACTTTCTTCATCC and AdhB_rev AAGCTCTTCACCCCAGCGCGCCGCGGAAGATCGCC) and cloned into the vectors pASG5 or pASG3, using the "Stargate" cloning system (IBA Lifesciences, Göttingen, Germany). The resulting plasmids code for fusion proteins of AdhB with N- or C-terminal Strep-tag sequences. The enzymes were subsequently produced in *E. coli* DH5α, which were grown in LB medium at room temperature and induced with added anhydrotetracycline as reported previously [4]. Cells were harvested by centrifugation and resuspended in two volumes of 10 mM Tris/HCl pH 7.5 containing 0.1 mg/ml DNase I. Cell-free extracts were prepared by sonification at 4°C, followed by ultracentrifugation (100,000 x g, 60 min). AdhB was exclusively present in the soluble fractions.

Protein purification and characterization. Cell-free extracts with overproduced AdhB were applied on a Strep-tag affinity column (IBA Lifesciences, Göttingen, Germany), and further purification of the proteins was performed as reported before [4]. Native molecular masses were determined by Ferguson plot analysis of AdhB after native polyacrylamide gel electrophoresis (6-10% polyacrylamide gels) and by crosslinking analysis with glutardialdehyde as described previously [12]. The buffer of the purified proteins was exchanged into protein storage buffer without the respective eluent (30 % glycerol, 150 mM NaCl, 25 mM Tris/Cl pH 7.9). Proteins were stored at -20°C until further use.

Cofactors were extracted from the purified AdhB protein by acid treatment with HCl and removing the precipitated protein by centrifugation. The supernatant was then analysed by UV-Vis spectroscopy. Further standard protein analytic techniques, such as SDS-PAGE and concentration determinations were performed as described in Coligan et al. [13].

Metal contents of protein fractions and controls were analysed by inductively coupled plasma mass spectrometry (ICP-MS) as described previously [14]; protein concentrations, were determined as described in Bradford [15]. The extracted cofactor was subjected to LC-MS/MS analysis [12].

LC-MS/MS measurements. LC-MS/MS measurements were performed on an Orbitrap ID-X (Thermo Scientific) connected to a Vanquish HPLC system (Thermo Scientific). The chromatographic separation was performed using a SeQuant ZIC-pHILIC column (150 × 2.1 mm, 5 µm particle size, peek coated, Merck) connected to a guard column of similar specificity (20 × 2.1 mm, 5 µm particle size, Phenomoenex) a constant flow rate of 0.1 ml/min with mobile phase A with mobile phase comprised of 10 mM ammonium acetate in water, pH 9, supplemented with medronic acid to a final concentration of 5 µM (A) and 10 mM ammonium acetate in 90:10 acetonitrile to water, pH 9,

 doi:10.20944/preprints202507.0481.v1

supplemented with medronic acid to a final concentration of 5 µM (B) at 40° C . The injection volume was 1 µl. The mobile phase profile consisted of the following steps and linear gradients: 0 – 1 min constant at 90 % B; 1 – 9 min from 90 to 40 % B; 9 to 10 min constant at 40 % B; 10 – 10.1 min from 40 to 90 % B; 10.1 to 20 min constant at 90 % B. 503.22, 541.175, 755.333, 793.289, 831.245

The Orbitrap ID-X was used in negative mode. Ionisation was performed using a high temperature electro spray ion source at a static spray voltage of 2500 V (negative), Sheath gas at 35 (Arb), Auxilary Gas at 7 (Arb), and Ion transfer tube and Vaporizer at 300 and 275°C. Data-dependent MS2 measurements were conducted applying an orbitrap mass resolution of 120000 using quadrupole isolation in a mass range of 500 – 1000 and combining it with a high-energy collision-induced dissociation (HCD). HCD was performed on five ions of interest, predefined in a target list (503.22, 541.175, 755.333, 793.289, 831.245) according to prior full scan runs, applying a mass tolerance of 25 ppm for precursor selection with a relative collision energy of 30 %. Fragments were detected using the ion-trap mass analyser. Acquired data was analysed qualitatively by generation of extracted ion chromatograms applying a mass tolerance of 5 ppm using QualBrowser (Thermo Scientific).

Enzymatic assays and product analysis. Enzyme activity was assayed in 100 mM HEPPS buffer at pH 8.,0. Routinely, activity was measured in a continuous photometric assay by directly following the formation of NADH at 340 nm (ε = 6.22 mM^{-1} cm^{-1}). The assay mixture contained AdhB (10-20 µg/ml),0.5 mM NAD^+ or NADH, respectively. The reactions were started by adding the respective substrates ethanol, propanol, acetaldehyde, or propionaldehyde (1 mM). Also tested but not accepted by AdhB were benzyl alcohol, butanol, 2-phenoxyethanol, pentanol, methanol, isopropanol, benzaldehyde, phenylacetaldehyde, and formaldehyde. For supplementation of Fe^{2+} ions, 100 µM iron-(II)-sulfate was used in the enzymatic assays. Tolerance to higher ethanol or n-propanol concentrations was tested accordingly. Inactivation of AdhB was fitted using an equation for exponential decay, according to $v = (V^0 - Plateau) * e^{-K\,[substrate]} + Plateau$; Michaelis-Menten enzyme kinetics with included substrate inhibition was calculated using the equation $v = \frac{V_{max} * [substrate]}{K_m + \frac{[substrate]}{1 + \frac{[substrate]}{K_i}}}$.

AdhB was used in a coupled assay with AOR as demonstrated with BADH [16]. 5-20 µg/ml of purified AOR and AdhB were mixed with 5 mM benzyl viologen, 1 mM NADH, and 10 mM acetic acid in 100 mM HEPPS buffer at pH 8.0 under anaerobic conditions (H_2:N_2 atmosphere; 2.5%:97.5%). Samples were incubated at 70°C for 5 minutes before ethanol detection to denature the enzymes AOR and AdhB.

Benzaldehyde and benzoate concentrations were determined via HPLC as published previously [16]. Ethanol was detected by the Megazyme ethanol detection kit (Wicklow, Ireland) following manufacturer's instructions, or by HPLC-RID on an Agilent Infinity 1260 HPLC system using a Rezex-ROA-Organic Acid H^+ (8%) column (50 x 7.8mm; Phenomenex, USA) at 60°C. Samples for HPLC analysis were collected for each time point and diluted in 1:1 ratio with sample buffer (0.005 N sulfuric acid in ddH_2O). Aliquots of 5 µl were analysed using 0.005 N sulfuric acid in ddH_2O as mobile phase in isocratic mode with a flow rate of 0,6 ml/min. Detection in RID was performed at 40°C (Retention times: ethanol 3.6 min, acetaldehyde 2.4 min, acetic acid 2.2 min).

Recombinant gene expression and growth conditions in *Aromatoleum* spp. The *adhB* gene of *A. aromaticum* EbN1 (ebA4623) was amplified via PCR with primers as stated above. The plasmid pASG103_AdhB was generated via Stargate cloning procedure, using a modified pASG103 vector (IBA Lifesciences, Göttingen, Germany) with a broad host range and a mob_ori- as published in [17,18]. The plasmid codes for AdhB with a C-terminal Twin-Strep-tag. Recombinant strains of *A. evansii* KB740 were generated by a conjugation procedure as published in [17].

For growth experiments, minimal TA media were used with individual carbon sources supplemented [18]. 5 mM succinate and varying concentrations of ethanol were used as carbon sources (1% ethanol corresponds to 17 mM). Strains under aerobic conditions were grown shaking at

 doi:10.20944/preprints202507.0481.v1

250 rpm at 28°C, strains under denitrifying conditions as standing cultures at 28°C. Expression of *adhB* in recombinant *A. evansii* strains was induced by adding 200 ng/ml anhydrotetracyclin.

Phylogeny and structure comparison. Proteins related to AdhB were identified by BLAST searches against the protein database and TBLASTn searches against the core_nucleotide database. Moreover, the phylogenetic position of AdhB and related proteins was determined by constructing a phylogenetic tree with various other members of the Fe-dependent alcohol dehydrogenase/dehydroquinate synthase superfamily (conserved domains category cl02872), which were aligned using Clustal Omega (www.ebi.ac.uk/Tools/msa/clustalo and avermitilis.ls.kitasato-u.ac.jp/clustalo) with bootstrap values calculated in 1000 replications. A neighbor-joining tree was constructed based on the alignment, using the Program iTOL (itol.embl.de/).

An Alphafold structure of AdhB is available from the uniprot database (Q5P150), which was structurally aligned to the closest known relatives with solved structures (PDB numbers 3OWO, 2BI4, 1RRM), using ChimeraX 1.9.

3. Results

3.1. AdhB Is an Alcohol Dehydrogenase for Small Aliphatic Alcohols

AdhB containing either an N- or C-terminal strep tag fusion was overproduced and purified from recombinant *E. coli* cells containing expression plasmids with the cloned *adhB* gene (ebA4623), using affinity chromatography. Homogeneous preparations were obtained with yields of 5 mg protein (l of culture)$^{-1}$ of the N-terminally or 10.5 mg protein l^{-1} of the C-terminally tagged variant (from 2 l of culture). Because of the higher yield, the C-terminally tagged variant was used for the further experiments. Starting with 786 mg of protein from 5 g wet cell mass, 8.6 mg of purified AdhB were obtained. While no activity was recorded in the cell extract, purified AdhB protein after affinity chromatography showed a specific activity of 16.2 ± 3.0 mU (mg protein)$^{-1}$, using ethanol and NAD^+ as substrates. Assays with $NADP^+$ replacing NAD^+ showed no activity.

AdhB consisted of a single subunit migrating at 40 kDa in SDS-PAGE, which fits to the expected mass of 40.4 kDa of the *adhB* gene product (including the strep-tag). The native mass was determined as 160 kDa by Ferguson plot analysis, suggesting a homotetrameric composition, which was confirmed by crosslinking studies with glutardialdehyde (Fig. 1).

 doi:10.20944/preprints202507.0481.v1

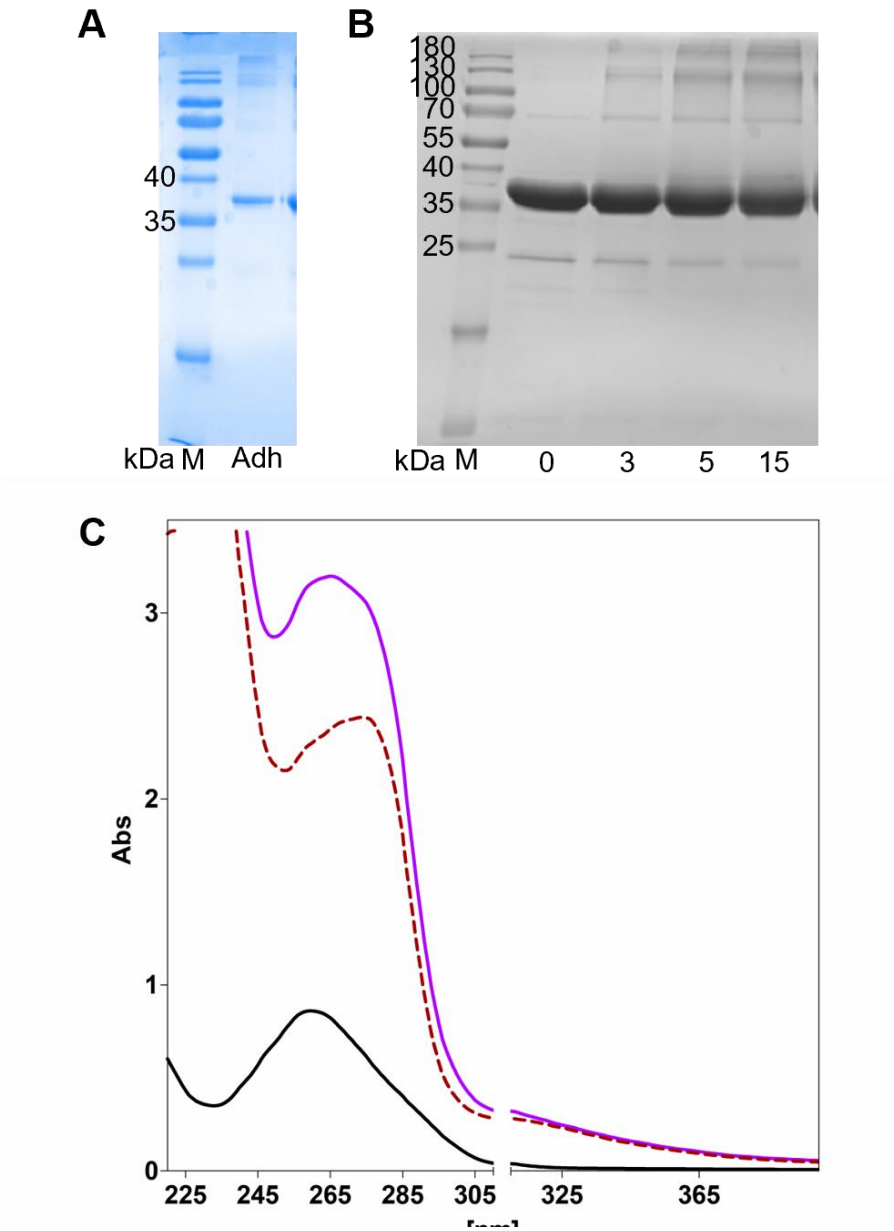

Figure 1. Molecular properties of AdhB. A: SDS-PAGE of purified recombinant AdhB. B: SDS-PAGE of crosslinked AdhB. Numbers refer to time incubated. C: UV-Vis spectra of AdhB, violet: AdhB protein, black: supernatant after protein precipitation by acid, orange: difference spectrum of AdhB and supernatant.

The UV-Vis spectrum of purified AdhB showed an unusually broad maximum around 270 nm and some residual absorption at 305 to 360 nm (Fig. 1C). The latter feature may be expected from an enzyme affiliated to the family III of Fe-dependent alcohol dehydrogenases, which often show a small peak at 330 nm due to the bound Fe^{2+} ion [19]. In contrast, the broad maximum ranging from 260 to 280 nm indicates the presence of an unknown cofactor, as recently observed for a benzyl alcohol dehydrogenase (BaDH) affiliated to the Zn-dependent family I after recombinant expression in *E. coli* [12]. As reported for BaDH, the cofactor can be extracted by acidic precipitation of the protein. After removing the protein by centrifugation, the supernatant exhibits an absorption maximum of 260 nm, suggesting a nucleotide-like molecule binding to the enzyme. We tried to evaluate its nature by high-resolution LC-MS/MS analysis of the supernatant and detected single-charged m/z ions of 831.2449, 793.2892, 755.3335, 514.1757, and 503.2201 in full scan runs. Fragmentation analysis targeting those ions revealed consistently appearing fragments of 251.2077 and 79.9770 m/z (see SI). As of now, we cannot correlate these data with any known molecule. Remarkably, some identical masses (particularly of the fragments) were recorded previously recorded for the molecule bound to BaDH

 doi:10.20944/preprints202507.0481.v1

[12], suggesting that carrying this molecule his may be a common phenomenon for recombinantly expressed proteins in *E. coli*. After subtracting the spectrum of the supernatant from the AdhB spectrum, the maximum is at 280 nm. The expected absorption value based on the protein sequence lies between the value as measured for AdhB and that of the difference spectrum (expected absorption of 2.62 vs. recorded values of 2.78 before and 2.28 after subtracting the absorption of the extracted cofactor).

Elemental analysis by ICP-MS showed the presence of 0.1 Fe, 0.06 Ni, and up to 0.13 Zn, as well as up to 1.9 P per subunit (table 1). This is consistent with the affiliation of AdhB with the family of Fe-dependent alcohol dehydrogenases, although Fe appears to be present at only 10% occupancy and may be partially substituted with Ni or Zn. Supplementation of Fe^{2+} to the enzyme preparation or the assay buffers did not show a beneficial effect on enzyme activity (data not shown). The presence of 1.9 P per subunit is consistent with a potential nucleotide-like cofactor bound to the enzyme.

Table 1. ICP-MS analysis of AdhB. Values are given in atoms of element (subunit of AdhB)$^{-1}$.

	desalted AdhB
Mg	0.01
P	1.88
Ca	0.03
Mn	0.02
Fe	0.10
Co	0.00
Ni	0.06
Cu	0.01
Zn	0.13
Se	0.00
Mo	0.00
W	0.00

The enzyme was assayed for activity with various alcohols and aldehydes, as well as NAD^+/NADH or $NADP^+$/NADPH. AdhB only showed activity with NAD^+ or NADH and the substrate spectrum was restricted to the oxidation of ethanol or *n*-propanol (specific activities 23 and 25 mU (mg protein)$^{-1}$) and to reduction of acetaldehyde or propionaldehyde (specific activities 161 and 123 mU (mg protein)$^{-1}$), using the respective substrates at 1 mM. Substrates not accepted by AdhB include methanol, *n*-butanol, *n*-pentanol, benzyl alcohol, 2-phenylethanol, isopropanol, formaldehyde, benzaldehyde, or phenylacetaldehyde. The pH dependency of the enzyme was determined in forward and reverse directions, using ethanol/NAD^+ and acetaldehyde/NADH as substrates. Ethanol oxidation rates by AdhB decreased with increasing pH values in the range of pH 6.0 -9.0, exhibiting about twofold lower rates at pH 9.0 than at pH 6.0, whereas the rates of acetaldehyde reduction increased about twofold between pH 6.0 and 8.5 and decreased again by ca. 20% at pH 9.0) (Fig. 2).

 doi:10.20944/preprints202507.0481.v1

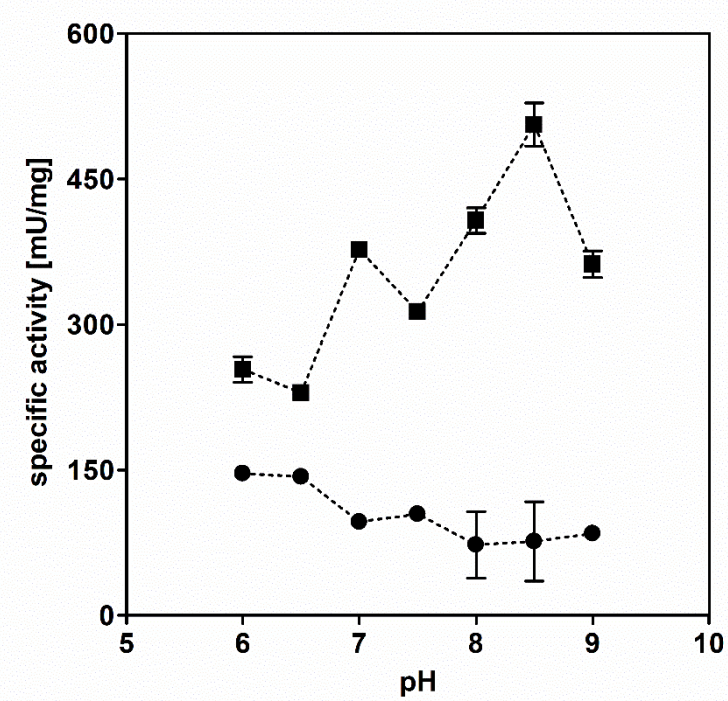

Figure 2. pH dependence of AdhB. The pH dependence of acetaldehyde reduction with NADH (circles) and of ethanol oxidation with NAD^+ (squares) is shown.

An enzyme kinetic analysis was performed for ethanol or *n*-propanol oxidation as well as for acetaldehyde and propionaldehyde reduction. As shown in Fig. 3, the data fitted to the Michaelis-Menten equation and revealed very similar behaviour for the C2- and C3-substrates (Table 3). AdhB showed similar apparent V_{max} values for aldehyde reduction and for alcohol oxidation, but the calculated apparent K_m values were much higher for alcohol oxidation than for aldehyde reduction (Table 2).

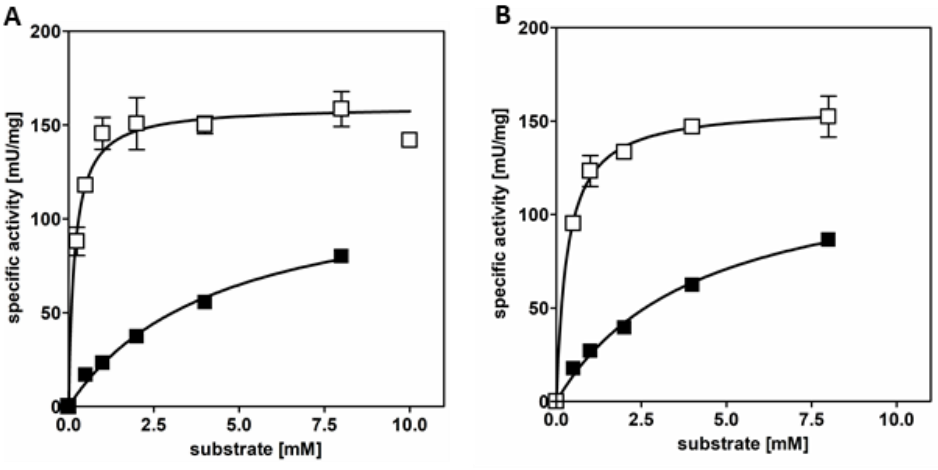

Figure 3: AdhB steady state kinetics. A: (white squares) reaction with acetaldehyde; (black squares) reaction with ethanol. B: (white squares) reaction with propionaldehyde; (black squares) reaction with n-propanol.

Table 2. Enzyme kinetics of purified AdhB.

substrate	ethanol	acetaldehyde	n-propanol	propionaldehyde
App. V_{max} [U/mg]	121.3	160.1	129.8	158.1
app. k_{cat} [s^{-1}]	79.7	105.1	85.2	103.8

 doi:10.20944/preprints202507.0481.v1

app.K_m [mM]	4.4	0.2	4.2	0.3
k_{cat}/K_m [mM^{-1} s^{-1}]	18.1	525.5	20.3	346.1

The discrepancy of the apparent K_m values of forward and backward reaction results in higher catalytic efficiencies (k_{cat}/K_m) of AdhB for aldehyde reduction than for alcohol oxidation. This feature of AdhB may provide a "safety valve" to prevent the production of high concentrations of toxic aldehydes.

3.2. Tolerance to Alcohols

To evaluate its applicability even in highly concentrated alcohol solutions, AdhB was tested for its tolerance to high ethanol or propanol concentrations. To this end, alcohol oxidation assays with NAD^+ have been set up with concentrations up to 40 % (v/v; equal to 6.9 M for ethanol). Remarkably, the enzyme appeared to be hardly affected by the alcohols up to 20%, exhibiting Michaelis-Menten-like kinetics with slight substrate inhibition. Only at over 20% (v/v) of ethanol or propanol, the activity of AdhB decreases exponentially with increasing alcohol concentrations, but still shows 9 % of its maximum activity at 40% (v/v) of ethanol and 22% of the maximum with propanol (Fig. 4). The apparent V_{max} (indicated as 100% relative activity) and K_m values were reasonably similar with those obtained from the study with lower substrate concentrations, except for a six-fold higher apparent K_m value for ethanol (24.9 mM), which is probably an artefact from the fewer data points obtained at low concentrations. Moreover, very weak substrate inhibition effects (K_i = 18 - 25 M) have been observed with both substrates, which are only visible in the analyses with high enough alcohol concentrations (Fig. 4).

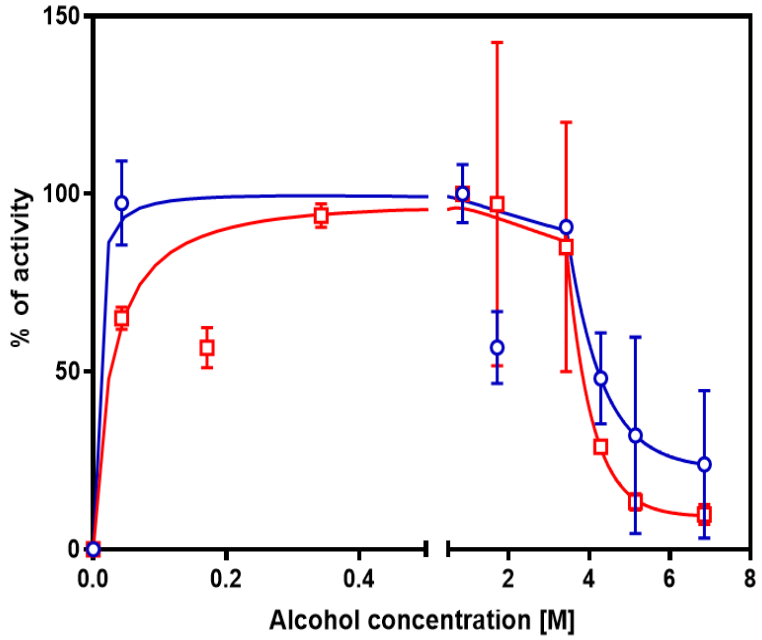

Figure 4. Tolerance of AdhB to high concentrations of alcohols. Data are shown for ethanol (red) and n-propanol (blue) as substrates.

3.3. AdhB Enables Aromatoleum evansii to Grow on Ethanol as Carbon Source

Utilisation of ethanol as sole carbon source has been reported for *A. aromaticum* EbN1, but the closely related species *A. evansii* KB740 has been reported unable to grow on this substrate [20,21]. A comparison of the respective genomes indeed showed that the *aldB-adhB* operon or comparable genes somewhere else on the chromosome are completely lacking in *A. evansii* (accession numbers GCA_000025965.1; GCA_012910805.1).

 doi:10.20944/preprints202507.0481.v1

Since *A. aromaticum* should be able to grow with ethanol as carbon source aerobically as well as under denitrifying conditions [22–24], we used the strain as a positive control for a complementation study in *A. evansii*. Since both species grow well on succinate, we used this substrate for additional control experiments (Figure 7A). We confirmed that *A. aromaticum* grows very well aerobically with either succinate or ethanol at different concentrations, ranging from 0.5 to 2% (w/v), while *A. evansii* only showed growth on succinate, but not on ethanol. However, if *A. evansii* expresses the *adhB* gene from *A. aromaticum* from an introduced plasmid, it shows an even better aerobic growth behaviour on ethanol than the latter. In both cases, growth rates were slightly reduced in the experiments with 2% ethanol, probably indicating substrate toxicity effects (Fig. 5). Under denitrifying conditions, the two control strains showed the same behaviour for growth on ethanol (growth of *A. aromaticum*, no growth of *A. evansii*), but the recombinant *A. evansii* cells carrying the *adhB* gene did not show reproducible growth on ethanol (data not shown), possibly because of the lack of a coexpressed *aldB* gene, which codes for the subsequent aldehyde dehydrogenase [4,5].

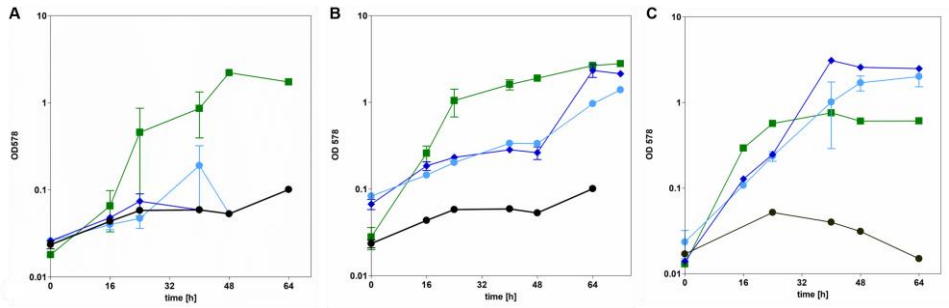

Figure 5. Aerobic growth of wild type *Aromatoleum* species compared to recombinant *A. evansii* KB740 expressing the *adhB* gene. Growth was recorded on succinate (green), 1% or 2% of ethanol (light or dark blue, respectively), and compared to controls without added substrates (grey). A: *A. evansii* KB740, B: *A. aromaticum* EbN1, C: recombinant *A. evansii* expressing *adhB*.

3.4. Application of AdhB in Coupled Enzyme Reactions

We used AdhB to develop potential applications for the enzyme-catalysed conversion of organic acids to alcohols, which may be used as biofuel components. To this end, we intended to set up a coupled reaction of the tungstoenzyme aldehyde oxidoreductase (AOR) [14,25] with AdhB, taking advantage of the special capability of AOR to simultaneously reduce many different non-activated acids to the respective aldehydes and NAD^+ to NADH. We already demonstrated the feasibility of this coupling in a previous report by reducing benzoate to benzyl alcohol with AOR and a benzyl alcohol dehydrogenase, which was driven by hydrogen as reductant [16]. In this study, we intended to use AOR to reduce acetate to acetaldehyde, which should be further reduced to ethanol by AdhB in an NADH-dependent reaction. Instead of using hydrogen as reductant, we tried two alternative electron donor systems for powering the reaction, either benzaldehyde as a sacrificial substrate or benzyl viologen pre-reduced by Ti(III)-citrate (Figure 8). Remarkably, we observed significant ethanol formation in both setups, demonstrating that either electron donor enables AOR to simultaneously reduce acetic acid to acetaldehyde and NAD^+ to NADH. Both the acetaldehyde and NADH intermediates produced by AOR are substrates for AdhB, which converts them to ethanol and NAD^+. Therefore, NAD^+ and NADH are continuously recycled between AOR and AdhB, and their ratio does not change very much during the course of the reactions [16].

The system driven by benzaldehyde showed a decrease of benzaldehyde to about half of the starting concentration within 60 min, while ethanol was simultaneously formed at about half of the rate of benzaldehyde decay (Fig. 6A). During the next 60 min, only a very small increase in ethanol and no further decrease of benzaldehyde were recorded, indicating that the system reached an equilibrium state. Remarkably, the NADH concentration showed some decrease during the second 60 min, but stayed almost the same during the first 60 min, indicating a highly efficient regeneration during the first phase via AOR-mediated benzaldehyde oxidation (Fig. 6A).

 doi:10.20944/preprints202507.0481.v1

The system driven by pre-reduced benzyl viologen (5 mM) showed continuous production of ethanol over 120 min coupled with an increase in NADH concentration. Since we have confirmed that AdhB is not able to use viologens as electron donors (data not shown), reduced benzyl viologen apparently acted as an electron donor for AOR, enabling it to reduce acetate to acetaldehyde and residual NAD^+ to NADH and providing AdhB with both substrates required for ethanol synthesis (Fig. 8B).

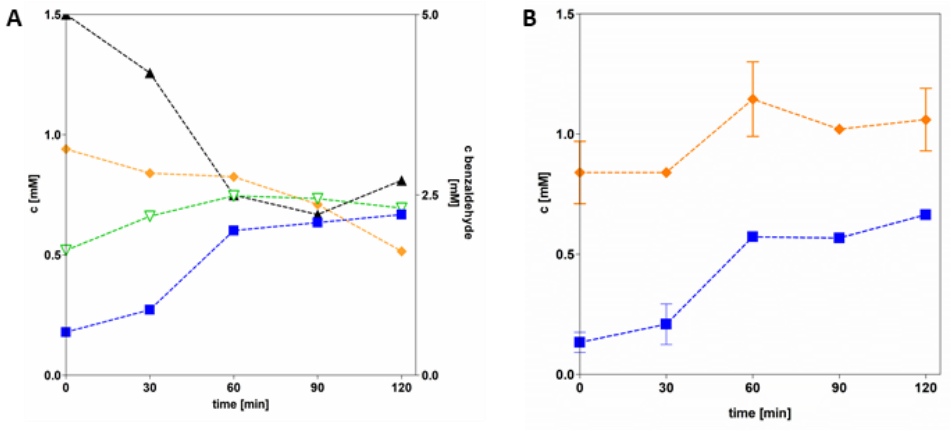

Figure 6. Reduction of acetic acid to ethanol. A: Cascade reaction system with sacrificial aldehyde (benzaldehyde, black graph), containing purified AOR and AdhB, NADH (orange) and acetic acid (10 mM). Formation of products and intermediates: ethanol (blue) and acetaldehyde (green). B: Cascade reaction system with reduced benzyl viologen (5mM), containing purified AOR and AdhB, NADH and acetic acid. Blue: concentration of produced ethanol, orange: concentration of NADH.

4. Discussion

We report here on AdhB from *A. aromaticum*, an NAD^+-dependent enzyme of the iron-dependent ADH family III which exhibits a very small substrate range, only catalysing the oxidation of ethanol and *n*-propanol or the reduction of the respective aldehydes, while it is not active on larger aliphatic, aromatic, or secondary alcohols. The enzyme seems to be highly deficient in the active site metal, as indicated by a relatively low specific activity and an iron content as low as 0.1 atoms per subunit. Therefore, only a fraction of the enzyme appears to be in the active, metal-bound state, even if it may also be active with Zn or Ni, which have been detected in substoichiometric amounts as well. The active-site Fe^{2+} could not be complemented with added Fe^{2+}, suggesting that metal incorporation may require special conditions, which are not met in the heterologous expression host.

AdhB shows a homotetrameric composition, which is in contrast to the homodimeric compositions of Adh II from *Zymomonas mobilis* [26] and 1,2- propanediol dehydrogenase from *E. coli* [27], or the decameric quaternary structure of 1,3-propanediol dehydrogenase from *Klebsiella pneumoniae* [28], which represent the closest related enzymes with known structures. AdhB and Adh II also appear to share retention of significant activity at high alcohol concentrations [29], with AdhB still showing normal enzyme kinetics up to 20% alcohol. While the UV-Vis spectrum of AdhB showed no evidence of a bound NAD^+ cofactor, the presence of an unknown nucleotide-like cofactor exhibiting an absorption maximum at 260 nm was detected in the purified protein. While we haven't been able to identify this cofactor yet, we have previously encountered the same situation in another alcohol dehydrogenase from *A. aromaticum* EbN1 that has been recombinantly produced in *E. coli* (Gemmecker et al. 2024). Therefore, the presence of this cofactor may actually be a common feature for recombinant NAD(P)-binding proteins produced in *E. coli*. We presume that this incident has become evident in working with AdhB or BaDH, because either of these proteins is completely devoid of any Trp residue, and they only contain the two Trp present in the twin strep-tag. This results in unusually low absorption peaks at 280 nm (extinction coefficients of AdhB: 8.94 and 19.94

 doi:10.20944/preprints202507.0481.v1

mM^{-1} cm^{-1} without and with twin-strep tag, respectively, for BaDH see [12]), which are getting more distorted by a cofactor absorbing at 260 nm than in an enzyme with a more usual Trp content.

BLAST analysis revealed that from the sequenced strains of the genus *Aromatoleum* (NCBI taxid 551759), only *Aromatoleum aromaticum* strains EbN1 and pCyN1 and *A. buckelii* strain U120 contain *adhB* orthologues and degrade ethanol. The same trait is found in a few close relatives affiliated to the species *Thauera aromatica* or *T. chlorobenzoica* (see table 3), indicating that *adhB* enables ethanol degradation in these strains. However, the other taxonomically described strains of the genera *Aromatoleum*, *Thauera* or *Azoarcus* are lacking orthologues of the *adhB* gene in their genomes, although some of them still grow on ethanol [22,30] (see table 3). Each of the latter strains contains at least two genes coding for uncharacterized "alcohol dehydrogenases" or "zinc-binding dehydrogenases", which may substitute for *adhB* in ethanol oxidation. *A. evansii* KB740 is one of the strains devoid of any gene coding for *adhB* or any Fe-ADH and is not growing on ethanol, although it contains 14 genes for predicted alcohol dehydrogenases from other families (coding for three Zn-dependent ADHs, six SDR, three S-(hydroxymethyl)glutathione dehydrogenases, one acryloyl-CoA reductase and one quinone oxidoreductase). We show here that recombinant expression of *adhB* from *A. aromaticum* is sufficient to enable *A. evansii* to grow on ethanol, confirming the proposed physiological role of the gene.

Table 3. Growth on ethanol and presence of *adhB* gene in the genus *Aromatoleum* and close relatives. +, positive; -, negative; ND, not determined.

organism	Growth on ethanol	*adhB* gene present (% protein identity)
A. aromaticum EbN1	+	+ (100)
A. aromaticum pCyN1	+	+ (100)
A. bremense PbN1	-	-
A. petrolei ToN1	+	-
Aromatoleum sp. strain EB1	ND	-
A. toluolicum T	+	-
A. diolicum 22Lin	-	-
A. evansii KB740	-	-
A. buckelii U120	+	+ (99)
A. anaerobium LuFRes1	+	-
A. tolulyticum Tol-4	+	-
A. toluvorans Td21	+	-
A. toluclasticum MF63	ND	-
Azoarcus indigens VB32	ND	-
Az. communis SWub3	+	-
Az. olearius BH72	+	-
Thauera aromatica K172/AR-1	+	+ (90)
T. chlorobenzoica 3CB1	ND	+ (90)
T. aromatica SP/LG356	ND	+ (89)

Synthetic pathways. Finally, we show here that AdhB may be applied as an auxiliary enzyme in synthetic pathways converting acetate or propionate to the corresponding alcohols, which may be used as fine chemicals or biofuels. An advantage of performing this reaction by coupling alcohol dehydrogenases with the tungsten enzyme AOR comes from the high versatility of AOR, both in

 doi:10.20944/preprints202507.0481.v1

regard to the range of acids reduced and different available sources of reducing equivalents [25]. We have shown previously that benzoate is converted to benzyl alcohol by AOR coupled to a benzyl alcohol dehydrogenase (BaDH), using H_2 as sole reductant for AOR, which exhibits H_2- oxidising hydrogenase side reactivity. This affords both reduction of benzoate to benzaldehyde and of NAD^+ to NADH by AOR, while BaDH reduces benzaldehyde further with NADH as reductant, closing the reaction cycle [16]. AOR has also been used in a different set-up to reduce acids in an electrochemical cell with electric current as reductant and hexamethyl viologen as very low-potential redox mediator ($E^{\circ\prime}$ = -610 mV) [31]. In this paper, we show that coupled assays with AOR and AdhB also convert acetate to ethanol with different reductants: either sacrificial aldehydes or even pre-reduced benzyl viologen (BV). While the first reaction may have been expected due to almost equivalent redox potentials of any acid/aldehyde pairs, the considerable production of ethanol with reduced BV has been unexpected because of the relatively high standard redox potential of BV ($E^{\circ\prime}$ = -374 mV). Other AORs have been reported to require more redox-negative electron donors such as reduced tetramethyl viologen ($E^{\circ\prime}$ = -536 mV) [32] or methyl viologen ($E^{\circ\prime}$ = -450 mV) [33] to afford acid reduction to the respective aldehyde. However, these considerations do not readily apply for the reaction observed here, which continues with reducing the aldehyde further to the alcohol. The calculated standard potentials of the redox pairs acetate/acetaldehyde ($E^{\circ\prime}$ = -0.588 mV) and acetaldehyde/ethanol ($E^{\circ\prime}$ = --0.202 mV) are almost equidistant to that of benzyl viologen (BV), resulting in an only slightly endergonic overall reaction according to the following equation:

$$\text{Acetate} + 4\ BV^{\bullet+} + 5\ H^+ \rightarrow \text{Ethanol} + 4\ BV^{2+} + H_2O,\ \Delta G^{\circ\prime} = +8.1\ \text{kJ mol}^{-1}.$$

Since the coupled reactions have been set up under conditions favouring the desired direction (e.g., with high acid concentrations), the calculated overall energetics is consistent with the observed BV_{red}-dependent production of ethanol. We assume that the structural details of the particular AOR used in these experiments contributes to its flexibility in accepting reductants with very different redox potentials. AOR from *A. aromaticum* consists of a basal FAD-containing AorC subunit, which forms a complex with several AorAB protomers, each containing a tungsten-cofactor and five Fe_4S_4 clusters. The AorAB protomers are stacked on top of AorC and each other, forming a filament-like quaternary structure where all redox cofactors are connected by electrically conductive chains of Fe_4S_4 clusters ("nanowires") [34]. Therefore, we propose that the actual redox state of AOR can be fine-tuned by either filling up or depleting the Fe_4S_4 clusters of the nanowires with electrons, enabling even relatively weak electron donors like BV_{red} to initiate the reaction, provided it is allowed by the overall thermodynamics. In the case of the coupled assay, the exergonic reduction reactions of NAD^+ (by AOR) and of the acetaldehyde intermediate (by AdhB) drive the endergonic reduction of acetate to acetaldehyde. Since all reactions occurring in the two enzymes are interdependent, the reaction system may be regarded as a special form of electron bifurcation [35].

In further refinement steps, the ethanol yield produced by the coupled system of AOR and AdhB may be increased further, both by optimising the biochemical parameters and by adding mechanical modules for continuous alcohol extraction, e.g. by pervaporation [36], membrane destillation [37], or vapor-phase membrane filtration [38].

Structure prediction of AdhB. An Alphafold prediction of the AdhB structure is available (Q5P150), which was compared to known structures of other Fe-ADHs by structural alignment. The closest structural matches have been found with Adh II from *Zymomonas mobilis* (3OWO; [26]) or lactaldehyde reductase FucO (1RRM or 2BI4; [27,39]) from *E. coli* (RMSD values 0.754, 1.131, and 1. 275 Å, respectively). An overlay of AdhB with Adh II is shown in Fig. 7, indicating highly similar structural properties of the enzymes, such as the metal-binding residues of the active site, Asp194, His198, His263, and His277. Additional amino acids surrounding the active site cavity and implied in substrate specificity of Adh II are completely conserved, including nonpolar (Phe149, Ile151, Ala162, Phe254, Leu259, and Ala361) and polar residues (His 267, Asp360, and Cys362). His 267 has been assigned a role in substrate binding and proton abstraction (with support from Asp361) and has been proposed to correctly position the substrates and restrict entrance of larger substrates, together with Phe149 and Phe254 [26]. Interestingly, most of these residues are also conserved in other

 doi:10.20944/preprints202507.0481.v1

members of the family that are specific for small alcohols, e.g., AdhE of *E. coli* [40]. Moreover, residues implicated in NAD^+ binding in Adh II or other related enzymes are highly conserved in AdhB, such as a Gly-rich pyrophosphate-binding motif at residues 96-99, a Thr138/Thr139 motif, and Leu 179 involved in binding the adenosine end of NAD^+, or Thr147/Phe149 binding the nicotinamide residue. Finally, AdhB also carries a conserved Asp39 residue, which is considered the major determinant for NAD^+ selectivity, while the $NADP^+$-dependent enzymes within the superfamily usually contain a Gly at this position [26].

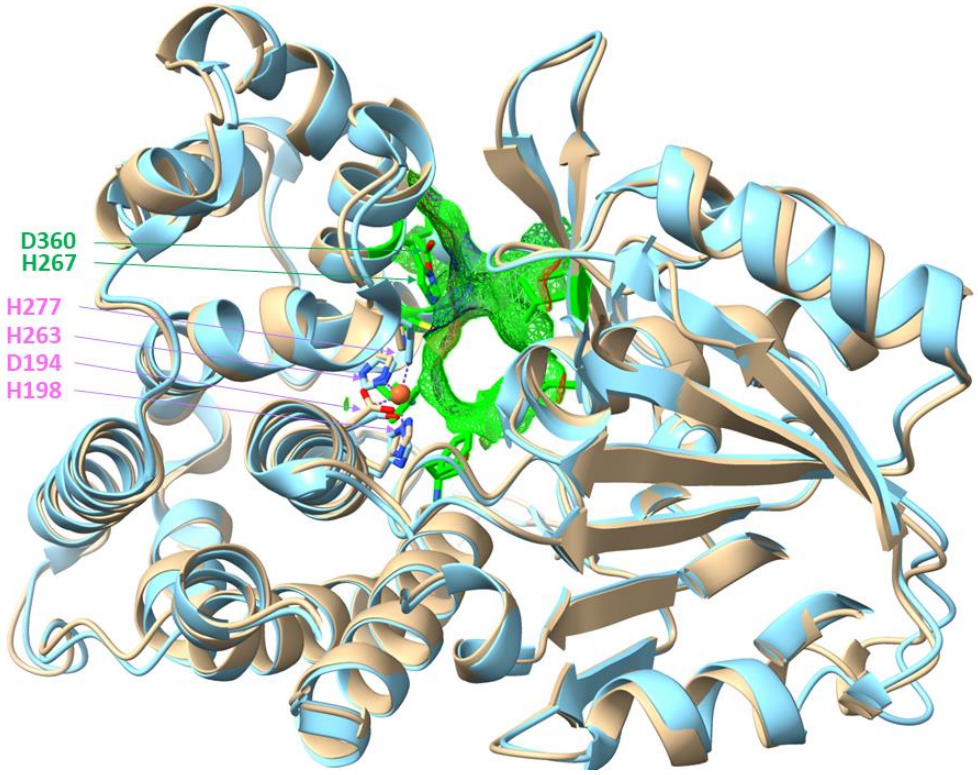

Figure 7. Overlay of the Alphafold prediction of an AdhB monomer (beige) with Adh II from *Zymomonas mobilis* (3OWO, cyan). The conserved residues binding the Fe^{2+} (orange ball) are shown from both overlaid structures (magenta), those forming the active site cavity only fom AdhB, together with the cavity surface (green; see text for additional residues). H267 and D360 are indicated as potential proton-abstracting residues.

Phylogenetic tree of the Fe-ADH superfamily. The phylogenetic position of AdhB was investigated by analysing the enzyme and some related proteins together with representatives of all subcategories of the Fe-ADH/dehydroquinate synthase superfamily (cl02872 in the conserved domains database). AdhB is affiliated to category cd08188, which includes other enzymes specific for short aliphatic alcohols like Adh II from *Z. mobilis* [41], but also 1,3-propanediol dehydrogenases involved in glycerol fermentation [42]. The structurally related lactaldehyde reductases (a.k.a. 1,2-propanediol dehydrogenases) are affiliated to the closely neighboring category cd08176 (Fig. 8). Fig. 8 also shows the principal division of the superfamily into 28 categories of "actual" Fe-ADHs, whereas three more basal categories contain the dehydroquinate and 2-deoxy-inosose synthases (DHQS-like; cd08169), glycerol-1-phosphate dehydrogenases (Gro1pDH-like; cd08549), and glycerol dehydrogenases (GroDH-like; cd08550). All four metal-binding residues are conserved in most of the Fe-ADH categories, except for the three basal groups and the four closest related categories (cd14864, 14866, 08192, and 08177). The three basal groups have completely or partially lost the first His of the metal-binding residues, and the Asp appears to be replaced by Glu in the DHQS-like proteins (cd08169). Category cd14864 represents proteins of unknown function from *Spirochaetes* containing none of the conserved residues, while the proteins of cd14866 are from halophilic bacteria, which may have adapted to high salt by replacing the Asp by Asn, as well as the first and last His by Lys and Gln, respectively. Finally, the maleylacetate reductases (MAR; cd08177) and the MAR-like

 doi:10.20944/preprints202507.0481.v1

proteins (cd08192) contain Asn and Arg, respectively, instead of Asp. Since all these exceptions are located at the base of the tree, AdhB is embedded in a part of the tree which likely contains exclusively active ADHs.

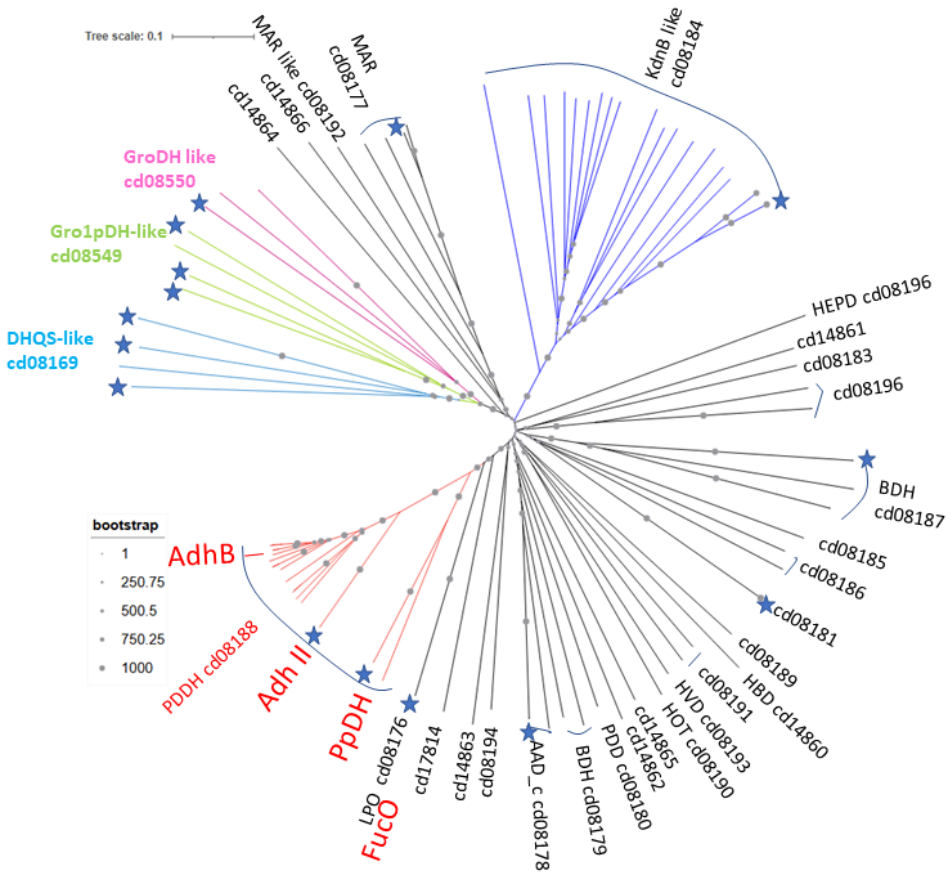

Figure 8. Phylogenetic tree of the Fe-ADH/dehydroquinate synthase superfamily. The positions of AdhB and a few other related enzymes are indicated. Asterisks indicate proteins with known structures. Abbreviations: DHQS, dihydroquinate synthase; Gro1pDH, glycerol-1-phosphate dehydrogenase (DH); GroDH, glycerol DH; MAR, maleylacetate reductase; KdnB, enzyme in 8-amino-3,8-didesoxy-octulosonate synthesis; HEPD, hydroxyethylphosphoate dehydrogenase; BDH, butanol DH; HBD, HVD, 5-hydroxyvalerate DH; HOT, hydroxyacid-oxoacid transhydrogenase; PPD, PDD, PDDH, 1,3-propanediol dehydrogenase-like; AAD_c, ADH domain of AdhE fusion protein; LPO, Lactaldehyde:propanediol oxidoreductase.

5. Conclusions

We show in this study that AdhB from *A. aromaticum* is an NAD^+-dependent ethanol dehydrogenase of the iron-dependent family III which only accepts ethanol or *n*-propanol as substrates and apparently is involved in the degradation on these alcohols. Expression of the corresponding gene even complements the related species *A. evansii* to growth on ethanol. The enzyme shows reasonable kinetic parameters for forward and reverse reactions, with significantly lower K_m values involved aldehyde reduction, and shows surprisingly high alcohol tolerance. Finally, we show that the enzyme can be used in a coupled reaction with the tungstoenzyme AOR to reduce acetate to ethanol.

Supplementary Materials: The following supporting information can be downloaded at the website of this paper posted on Preprints.org.

Author Contributions: Conceptualization, J.H. and Y.G.; methodology, Y.G., I.S., A.S. and N.P.; software, J.H. and Y.G.; validation, J.H., Y.G., A.S. and N.P.; formal analysis, J.H.; investigation, Y.G., I.S. and J.H.; resources, X.X.; data curation, X.X.; writing—original draft preparation, X.X.; writing—review and editing, X.X.;

 doi:10.20944/preprints202507.0481.v1

visualization, Y.G. and J.H.; supervision, J.H.; project administration, J.H.; funding acquisition, J.H. All authors have read and agreed to the published version of the manuscript.

Funding: This work was supported by the Deutsche Forschungsgemeinschaft (DFG grant He2190/15-1).

Data Availability Statement: All relevant data for this study are either shown in the paper or are available in the resources stated in the text.

Acknowledgments: We acknowledge Paula Oppong-Nti for contributions in the early state of this project.

Conflicts of Interest: The authors declare no conflicts of interests. .

Abbreviations

The following abbreviations are used in this manuscript:

MDPI	Multidisciplinary Digital Publishing Institute
AdhB	Fe-dependent alcohol dehydrogenase from *A. aromaticum*
NAD(P)	Nicotinamide adenine dinucleotide (phosphate)
Pdh	Phenylacetaldehyde dehydrogenase
ADH	Alcohol dehydrogenase
SDR	Short chain dehydrogenase/reductase
UV-Vis	Ultraviolet-visible light
SDS-PAGE	Sodium dodecylsulfonate polyacrylamide gel electrophoresis
ICP-MS	Inductively coupled plasma-mass spectrometry
LC-MS/MS	Liquid chromatography-double mass spectrometry
Tris	Tris-(hydroxymethyl)aminomethan
HEPPS	4-(Hydroxyethyl)-piperazine-1-propansulfonate
AOR	Aldehyde oxidoreductase
HPLC	High performance liquid chromatography
RID	Refractive index detector
PCR	Polymerase chain reaction
TA	*Thauera aromatica* medium
Da	Dalton
BaDH	Benzyl alcohol dehydrogenase
V_{max}	Michaelis-Menten maximum activity
K_m	Michaelis-Menten constant
BV	Benzyl viologen
FAD	Flavin adenine dinucleotide
DHQS	Dehydroquinate synthase
Gro1pDH	Glycerol-1-phosphate dehydrogenase
GroDH	Glycerol- dehydrogenase

References

1. Rabus, R.; Kube, M.; Heider, J.; Beck, A.; Heitmann, K.; Widdel, F.; Reinhardt, R. The Genome Sequence of an Anaerobic Aromatic-Degrading Denitrifying Bacterium, Strain EbN1. *Archives of Microbiology* **2005**, *183*, 27–36, doi:10.1007/s00203-004-0742-9.
2. Becker, P.; Wünsch, D.; Wöhlbrand, L.; Neumann-Schaal, M.; Schomburg, D.; Rabus, R. The Catabolic Network of Aromatoleum Aromaticum EbN1T. *Microbial physiology* 2024, *34*.
3. Rabus, R. Functional Genomics of an Anaerobic Aromatic-Degrading Denitrifying Bacterium, Strain EbN1. *Applied Microbiology and Biotechnology* 2005, *68*, 580–587.
4. Schmitt, G.; Arndt, F.; Kahnt, J.; Heider, J. Adaptations to a Loss-of-Function Mutation in the Betaproteobacterium *Aromatoleum Aromaticum*: Recruitment of Alternative Enzymes for Anaerobic Phenylalanine Degradation. *Journal of Bacteriology* **2017**, *199*, e00383-17, doi:10.1128/JB.00383-17.
5. Hege, D.; Gemmecker, Y.; Schall, I.; Oppong-Nti, P.; Schmitt, G.; Heider, J. Single Amino Acid Exchanges Affect the Substrate Preference of an Acetaldehyde Dehydrogenase. *Applied Microbiology and Biotechnology* **2025**, *109*, 103.

 doi:10.20944/preprints202507.0481.v1

6. Heider, J.; Hege, D. The Aldehyde Dehydrogenase Superfamilies: Correlations and Deviations in Structure and Function. *Applied Microbiology and Biotechnology* **2025**, *109*, 106, doi:0.1007/s00253-025-13467-5.
7. Conway, T.; Sewell, G.W.; Osman, Y.A.; Ingram, L.O. Cloning and Sequencing of the Alcohol Dehydrogenase II Gene from Zymomonas Mobilis. *Journal of Bacteriology* **1987**, *169*, 2591–2597, doi:10.1128/jb.169.6.2591-2597.1987.
8. Ingram, L.O.; Conway, T.; Clark, D.P.; Sewell, G.W.; Preston, J.F. Genetic Engineering of Ethanol Production in Escherichia Coli. *Applied and environmental microbiology* **1987**, *53*, 2420–2425, doi:10.1128/aem.53.10.2420-2425.1987.
9. Reid, M.F.; Fewson, C.A. Molecular Characterization of Microbial Alcohol Dehydrogenases. *Critical Reviews in Microbiology* **1994**, *20*, 13–56, doi:10.3109/10408419409113545.
10. Hernández-Tobías, A.; Julián-Sánchez, A.; Piña, E.; Riveros-Rosas, H. Natural Alcohol Exposure: Is Ethanol the Main Substrate for Alcohol Dehydrogenases in Animals? In Proceedings of the Chemico-Biological Interactions; 2011; Vol. 191, pp. 14–25.
11. Gaona-López, C.; Julián-Sánchez, A.; Riveros-Rosas, H. Diversity and Evolutionary Analysis of Iron-Containing (Type-III) Alcohol Dehydrogenases in Eukaryotes. *PLoS ONE* **2016**, *11*, doi:10.1371/journal.pone.0166851.
12. Gemmecker, Y.; Winiarska, A.; Hege, D.; Kahnt, J.; Seubert, A.; Szaleniec, M.; Heider, J. A PH-Dependent Shift of Redox Cofactor Specificity in a Benzyl Alcohol Dehydrogenase of <i>Aromatoleum Aromaticum<i> EbN1. *Applied Microbiology and Biotechnology* **2024**, *108*, s00253-024.
13. Coligan, J.E., Dunn, B.M., Ploegh, H.L., Speicher, D.W., Wingfield, P.T. *Current Protocols in Protein Science*; Coligan, J.E., Dunn, B.M., Ploegh, H.L., Speicher, D.W., Wingfield, P.T., Ed.; Wiley: New York, NY, 2001;
14. Arndt, F.; Schmitt, G.; Winiarska, A.; Saft, M.; Seubert, A.; Kahnt, J.; Heider, J. Characterization of an Aldehyde Oxidoreductase from the Mesophilic Bacterium *Aromatoleum Aromaticum* EbN1, a Member of a New Subfamily of Tungsten-Containing Enzymes. *Frontiers in Microbiology* **2019**, *10*, 71, doi:10.3389/fmicb.2019.00071.
15. Bradford, M.M. A Rapid and Sensitive Method for the Quantitation of Microgram Quantities of Protein Utilizing the Principle of Protein-Dye Binding. *Analytical Biochemistry* **1976**, *72*, 248–254, doi:10.1016/0003-2697(76)90527-3.
16. Winiarska, A.; Hege, D.; Gemmecker, Y.; Kryściak-Czerwenka, J.; Seubert, A.; Heider, J.; Szaleniec, M. Tungsten Enzyme Using Hydrogen as an Electron Donor to Reduce Carboxylic Acids and NAD+. *ACS Catalysis* **2022**, *12*, 8707–8717, doi:10.1021/acscatal.2c02147.
17. Salii, I.; Szaleniec, M.; Zein, A.A.; Seyhan, D.; Sekuła, A.; Schühle, K.; Kaplieva-Dudek, I.; Linne, U.; Meckenstock, R.U.; Heider, J. Determinants for Substrate Recognition in the Glycyl Radical Enzyme Benzylsuccinate Synthase Revealed by Targeted Mutagenesis. *ACS Catalysis* **2021**, *11*, 3361–3370, doi:10.1021/acscatal.0c04954.
18. Hege, D.; Gemmecker, Y.; Clermont, L.; Aleksic, I.; Olesky, G.; Szaleniec, M.; Heider, J. Genetic Manipulation of the Betaproteobacterial Genera Thauera and Aromatoleum. *Methods in Enzymology* **2025**, *714*, 139–161, doi:10.1016/bs.mie.2025.01.009.
19. Liang, F.; Sun, S.; Zhou, Y.; Peng, T.; Xu, X.; Li, B.; Tan, G. Escherichia Coli Alcohol Dehydrogenase YahK Is a Protein That Binds Both Iron and Zinc. *PeerJ* **2024**, *12*, e18040, doi:10.7717/peerj.18040.
20. Rabus, R.; Wöhlbrand, L.; Thies, D.; Meyer, M.; Reinhold-Hurek, B.; Kampfer, P. Aromatoleum Gen. Nov., a Novel Genus Accommodating the Phylogenetic Lineage Including Azoarcus Evansii and Related Species, and Proposal of Aromatoleum Aromaticum Sp. Nov., Aromatoleum Petrolei Sp. Nov., Aromatoleum Bremense Sp. Nov., Aromatoleum Toluolicum Sp. Nov. and Aromatoleum Diolicum Sp. Nov. *International Journal of Systematic and Evolutionary Microbiology* **2019**, *69*, doi:10.1099/ijsem.0.003244.
21. Anders, H.J.; Kaetzke, A.; Kampfer, P.; Ludwig, W.; Fuchs, G. Taxonomic Position of Aromatic-Degrading Denitrifying Pseudomonad Strains K 172 and KB 740 and Their Description as New Members of the Genera Thauera, as Thauera Aromatica Sp. Nov., and Azoarcus, as Azoarcus Evansii Sp. Nov., Respectively, Members of The . *International Journal of Systematic Bacteriology* **1995**, *45*, 327–333, doi:10.1099/00207713-45-2-327.

 doi:10.20944/preprints202507.0481.v1

22. Rabus, R.; Wöhlbrand, L.; Thies, D.; Meyer, M.; Reinhold-Hurek, B.; Kampfer, P. *Aromatoleum* Gen. Nov., a Novel Genus Accommodating the Phylogenetic Lineage Including *Azoarcus Evansii* and Related Species, and Proposal of *Aromatoleum Aromaticum* Sp. Nov., *Aromatoleum Petrolei* Sp. Nov.,<i> Aromatoleum Bremense. *International Journal of Systematic and Evolutionary Microbiology* **2019**, *69*, 982–997, doi:10.1099/ijsem.0.003244.
23. Rabus, R.; Widdel, F. Anaerobic Degradation of Ethylbenzene and Other Aromatic Hydrocarbons by New Denitrifying Bacteria. *Archives of Microbiology* **1995**, *163*, 96–103, doi:10.1007/BF00381782.
24. Rabus, R.; Widdel, F. Utilization of Alkylbenzenes during Anaerobic Growth of Pure Cultures of Denitrifying Bacteria on Crude Oil. *Applied and Environmental Microbiology* **1996**, *62*, 1238–1241, doi:10.1128/aem.62.4.1238-1241.1996.
25. Szaleniec, M.; Heider, J. Obligately Tungsten-Dependent Enzymes─Catalytic Mechanisms, Models and Applications. *Biochemistry* **2025**, *64*, 2154–2174, doi:10.1021/acs.biochem.5c00116.
26. Moon, J.H.; Lee, H.J.; Park, S.Y.; Song, J.M.; Park, M.Y.; Park, H.M.; Sun, J.; Park, J.H.; Kim, B.Y.; Kim, J.S. Structures of Iron-Dependent Alcohol Dehydrogenase 2 from Zymomonas Mobilis ZM4 with and without NAD+ Cofactor. *Journal of Molecular Biology* **2011**, *407*, doi:10.1016/j.jmb.2011.01.045.
27. Montella, C.; Bellsolell, L.; Pérez-Luque, R.; Badía, J.; Baldoma, L.; Coll, M.; Aguilar, J. Crystal Structure of an Iron-Dependent Group III Dehydrogenase That Interconverts L-Lactaldehyde and L-1,2-Propanediol in Escherichia Coli. *Journal of Bacteriology* **2005**, *187*, 4957–4966, doi:10.1128/JB.187.14.4957-4966.2005.
28. Marçal, D.; Rêgo, A.T.; Carrondo, M.A.; Enguita, F.J. 1,3-Propanediol Dehydrogenase from Klebsiella Pneumoniae: Decameric Quaternary Structure and Possible Subunit Cooperativity. *Journal of Bacteriology* **2009**, *191*, doi:10.1128/JB.01077-08.
29. O'Mullan, P.J.; Buchholz, S.E.; Chase, T.; Eveleigh, D.E. Roles of Alcohol Dehydrogenases of Zymomonas Mobilis (ZADH): Characterization of a ZADH-2-Negative Mutant. *Applied Microbiology and Biotechnology* **1995**, *43*, doi:10.1007/BF00164772.
30. Weiten, A.; Kalvelage, K.; Becker, P.; Reinhardt, R.; Hurek, T.; Reinhold-Hurek, B.; Rabus, R. Complete Genomes of the Anaerobic Degradation Specialists Aromatoleum Petrolei ToN1Tand Aromatoleum Bremense PbN1T. *Microbial Physiology* **2021**, *31*, 16–35, doi:10.1159/000513167.
31. Luo, S.; Adam, D.; Giaveri, S.; Barthel, S.; Cestellos-Blanco, S.; Hege, D.; Paczia, N.; Castañeda-Losada, L.; Klose, M.; Arndt, F.; et al. ATP Production from Electricity with a New-to-Nature Electrobiological Module. *Joule* **2023**, *7*, 1745–1758, doi:10.1016/j.joule.2023.07.012.
32. White, H.; Strobl, G.; Feicht, R.; Simon, H. Carboxylic Acid Reductase: A New Tungsten Enzyme Catalyses the Reduction of Non-activated Carboxylic Acids to Aldehydes. *European Journal of Biochemistry* **1989**, *184*, 89–96, doi:10.1111/j.1432-1033.1989.tb14993.x.
33. Heider, J.; Ma, K.; Adams, M.W.W. Purification, Characterization, and Metabolic Function of Tungsten-Containing Aldehyde Ferredoxin Oxidoreductase from the Hyperthermophilic and Proteolytic Archaeon *Thermococcus* Strain ES-1. *Journal of Bacteriology* **1995**, *177*, 4757–4764, doi:10.1128/jb.177.16.4757-4764.1995.
34. Winiarska, A.; Ramírez-Amador, F.; Hege, D.; Gemmecker, Y.; Prinz, S.; Hochberg, G.; Heider, J.; Szaleniec, M.; Schuller, J.M. A Bacterial Tungsten-Containing Aldehyde Oxidoreductase Forms an Enzymatic Decorated Protein Nanowire. *Science Advances* **2023**, *9*, eadg668, doi:10.1126/sciadv.adg6689.
35. Buckel, W.; Thauer, R.K. Energy Conservation via Electron Bifurcating Ferredoxin Reduction and Proton/Na^+ Translocating Ferredoxin Oxidation. *Biochimica et Biophysica Acta - Bioenergetics* **2013**, *1827*, 94–113, doi:10.1016/j.bbabio.2012.07.002.
36. Golubev, G.S.; Borisov, I.L.; Volkov, V. V. Thermopervaporative Removal of Isopropanol and Butanol from Aqueous Media Using Membranes Based on Hydrophobic Polysiloxanes. *Petroleum Chemistry* **2018**, *58*, 975–982, doi:10.1134/S0965544118110014.
37. Alkhudhiri, A.; Darwish, N.; Hilal, N. Membrane Distillation: A Comprehensive Review. *Desalination* 2012, *287*, 2–18.
38. Shalygin, M.G.; Kozlova, A.A.; Heider, J.; Sapegin, D.A.; Netrusov, A.A.; Teplyakov, V. V. Polymeric Membranes for Vapor-Phase Concentrating Volatile Organic Products from Biomass Processing. *Membranes and Membrane Technologies* **2023**, *5*, 55–67, doi:10.1134/S2517751623010055.

 doi:10.20944/preprints202507.0481.v1

39. Zavarise, A.; Sridhar, S.; Kiema, T.R.; Wierenga, R.K.; Widersten, M. Structures of Lactaldehyde Reductase, FucO, Link Enzyme Activity to Hydrogen Bond Networks and Conformational Dynamics. *FEBS Journal* **2023**, *290*, doi:10.1111/febs.16603.
40. Extance, J.; Crennell, S.J.; Eley, K.; Cripps, R.; Hough, D.W.; Danson, M.J. Structure of a Bifunctional Alcohol Dehydrogenase Involved in Bioethanol Generation in Geobacillus Thermoglucosidasius. *Acta Crystallographica Section D: Biological Crystallography* **2013**, *69*, 2104–2115, doi:10.1107/S0907444913020349.
41. Kinoshita, S.; Kakizono, T.; Kadota, K.; Das, K.; Taguchi, H. Purification of Two Alcohol Dehydrogenases from Zymomonas Mobilis and Their Properties. *Applied Microbiology and Biotechnology* **1985**, *22*, doi:10.1007/BF00252025.
42. Sun, S.; Shu, L.; Lu, X.; Wang, Q.; Tišma, M.; Zhu, C.; Shi, J.; Baganz, F.; Lye, G.J.; Hao, J. 1,2-Propanediol Production from Glycerol via an Endogenous Pathway of Klebsiella Pneumoniae. *Applied Microbiology and Biotechnology* **2021**, *105*, doi:10.1007/s00253-021-11652-w.